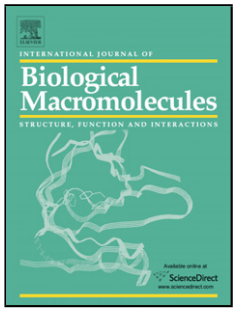

Title: Chitosan-based nanoparticles for rosmarinic acid ocular delivery - *in vitro* tests

Author: Sara Baptista da Silva Domingos Ferreira Manuela Pintado Bruno Sarmento

PII: S0141-8130(15)30169-0
DOI: http://dx.doi.org/doi:10.1016/j.ijbiomac.2015.11.070
Reference: BIOMAC 5575

To appear in: *International Journal of Biological Macromolecules*

Received date: 18-8-2015
Revised date: 16-11-2015
Accepted date: 25-11-2015

Please cite this article as: S.B. Silva, D. Ferreira, M. Pintado, B. Sarmento, Chitosan-based nanoparticles for rosmarinic acid ocular delivery - *in vitro* tests, *International Journal of Biological Macromolecules* (2015), http://dx.doi.org/10.1016/j.ijbiomac.2015.11.070

Chitosan-based nanoparticles for rosmarinic acid ocular delivery - *in vitro* tests

Sara Baptista da Silva[1,2*], Domingos Ferreira[1], Manuela Pintado[2], Bruno Sarmento[3,4*]

[1]-Laboratory of Pharmaceutical Technology, Department of Drug Sciences, Faculty of Pharmacy, University of Porto, Rua Jorge Viterbo Ferreira 228, 4050-313 Porto, Portugal

[2]-CBQF – Centro de Biotecnologia e Química Fina – Laboratório Associado, Escola Superior de Biotecnologia, Universidade Católica Portuguesa/Porto, Rua Arquiteto Lobão Vital, Apartado 2511, 4202-401 Porto, Portugal

[3]-CESPU, IINFACTS, Department of Pharmaceutical Sciences, Institute of Health Sciences-North, Rua Central de Gandra, 1317, 4585-116 Gandra, Portugal

[4]-INEB, Institute of Biomedical Engineering, University of Porto, Rua do Campo Alegre, 823, 4150-180 Porto, Portugal

[*] Corresponding author. Tel.: +351 220 428 500

E-mail address:

sara.baptistadasilva@gmail.com;

bruno.sarmento@ineb.up.pt;

Abstract

In this study, chitosan nanoparticles were used to encapsulate antioxidant rosmarinic acid, *Salvia officinalis* (sage) and *Satureja montana* (savory) extracts as rosmarinic acid natural vehicles. The nanoparticles were prepared by ionic gelation using chitosan and sodium tripolyphosphate (TPP) in a mass ratio of 7:1, at pH 5.8. Particle size distribution analysis and transmission electron microscopy (TEM) confirmed the size ranging from 200 to 300 nm, while surface charge of nanoparticles ranged from 20 to 30 mV. Nanoparticles demonstrate to be safe without relevant cytotoxicity against retina pigment epithelium (ARPE-19) and human cornea cell line (HCE-T). The permeability study in HCE monolayer cell line showed an apparent permeability coefficient P_{app} of 3.41 ± 0.99 x 10^{-5} and 3.24 ± 0.79 x 10^{-5} cm/s for rosmarinic acid loaded chitosan nanoparticles and free in solution, respectively. In ARPE-19 monolayer cell line the P_{app} was 3.39 ± 0.18 x 10^{-5} and 3.60 ± 0.05 x 10^{-5} cm/s for rosmarinic acid loaded chitosan nanoparticles and free in solution, respectively. Considering the mucin interaction method, nanoparticles indicate mucoadhesive proprieties suggesting an increased retention time over the ocular mucosa after instillation. These nanoparticles may be promising drug delivery systems for ocular application in oxidative eye conditions.

Keywords: Chitosan, nanoparticles, rosmarinic acid, cell models

1. Introduction

The ocular drug delivery is one of the major challenges in pharmaceutical sciences [1, 2]. Topical eye drop is the most convenient and comfortable route for ocular drug administration for patients. Nonetheless, it is well known that the delivery of drugs to targeted posterior ocular tissues is restricted by various precorneal, dynamic and static ocular barriers [3, 4]. In the past two decades,

ocular drug delivery research was focused on developing novel, safe and patient compliant formulations that may overcome these barriers and maintain higher drug levels in tissues. There are many described categories of ocular diseases, such as retinitis pigmentosa, glaucoma, cataracts, macular degeneration, retinoblastoma and diabetic retinopathy [5]. However, the etiology of these degenerative diseases remains poorly explained, thus mainly associated to light-mediated oxidative damage, PUFA content, environmental chemicals and the physical abrasion [6]. All these factors contribute to OS that may be seen as the key factor for ocular conditions [7]. OS is now associated to the disruption of blood-retinal barrier, apoptotic loss of retinal capillary cells, microvascular abnormalities, retinal neovascularization, oxidative modified DNA, as well as suppression of antioxidants systems [8]. For this reason, the use of appropriate antioxidants may have potential on the metabolic and functional abnormalities in retinopathies [9, 10]. Rosmarinic acid is a potent antioxidant highly related to anti-angiogenic activity to retinal neovascularization in a mouse model of retinopathy [11]. Evidences demonstrated a significant inhibition of retinal endothelial cells proliferation in a dose-dependent manner, and an *in vitro* inhibition of tube formation angiogenesis. Additionally, rosmarinic acid showed no retinal toxicity. These data suggest rosmarinic acid could be a potent inhibitor of retinal neovascularization and may be applied in the treatment of vasoproliferative retinopathies [11]. It is also the major component of *Salvia officinalis* (sage) and *Satureja montana* (savory) natural extracts. The major biological activities of these plants often used in traditional medicine are highly related to contents of rosmarinic acid and the presence of other relevant phenolic compounds such as quercetin and rutin [12, 13] (such as: anti-diarrhea vector, digestion adjuvant, contribute to heal wounds, play an anti-inflammatory role, disinfectant, fight insomnia and decrease blood pressure). Beyond the biological huge benefits, antioxidants are extremely sensitive to light, oxygen, are highly reactive with other compounds, in some cases possess poor solubility, inefficient permeability, and are extremely unstable [14-16]. In this context, the delivery of antioxidants using the conventional dosage forms is challenging due to their low permeability, high instability and the losses during metabolism before reaching systemic circulation [17]. Nanotechnologies as ocular drug delivery systems are one of the most interesting and challenging

endeavors, due to the eye critical environment [2]. In the case of ophthalmic nano-drug delivery systems, it is crucial to evaluate an appropriate particle size and a narrow size range, ensuring low irritation, adequate bioavailability and compatibility with ocular tissues [18]. Nanotechnologies together with the implementation of optimal, non-invasive and painless administration routes have been deeply studied, considering different biodegradable polymers, their core proprieties and mucosa interaction [4]. Chitosan is a positively charged polysaccharide which binds to negatively charged corneal surface, with potential to improve precorneal residence and decrease clearance [19]. However, for using chitosan as a base material to produce nanoparticles with application in biomedical sciences, it is essential to evaluate their bioavailability, cytotoxicity and capacity of transporting bioactive molecules. For this purpose, *in vitro* cell culture models may be considered as the most useful technique to better predict the permeability/absorption of bioactive compounds. Ocular cell-based models (retina pigment epithelium (ARPE-19) and human cornea cell line (HCE-T)) have been used for numerous other purposes, such as studying passive and active transport of drugs and endogenous substances, cellular physiology, metabolism and protein expression, development of delivery systems for genes and antisense oligonucleotides, and cytotoxicity [20]. Both cell lines have been deeply evaluated for drug permeation studies [21, 22].The main aim of this study was to evaluate the safety performance, mucoadhesiveness, permeability and applicability potential in ocular cell-based models of chitosan nanoparticles encapsulating rosmarinic acid, sage and savory lyophilized extracts as rosmarinic carriers.

2. Materials and Methods

2.1. Materials and cells

Chitosan low molecular weight (≈50 kDa) with deacetylation degree of 86%, and sodium tripolyphosphate (TPP) were purchased from Sigma-Aldrich (Portugal). Stock solution of chitosan (1% *w/v*) were dissolved in 1% (*v/v*) acetic acid

solution and deionized water followed by filtration using a Millipore #2 paper filter and stored at 4 °C. TPP (0.1% *w/v*) were also dissolved in deionized water and stored in the same conditions. Two plants were selected as extract source namely S*alvia officinalis* (sage) and *Satureja montana* (savory), both provided by ERVITAL (Castro Daire, Portugal). These plants had been cultivated as organic products, and were supplied in their commercial form of dried leaves. After the crude plant sedimentation, samples were filtered and maintained at -80°C, for lyophilization procedures (Heto Holten A/S Drywinner). Then, solutions of 1% (*w/v*) of lyophilized powder were dissolved in deionized water followed by filtration using a Millipore #2 paper filter and stored at -20 ºC, as previously described [23, 24]. ARPE-19 and HCE-T human cell lines were obtained from the American Type Culture Collection (ATCC) and used at passages 14-35 and 18-32, respectively. Dulbecco's Modified Eagle Medium (DMEM), fetal bovine serum (FBS), L-glutamine, non-essential amino acids, and 100 U/mL penicillin and 100 mg/mL streptomycin, trypsin-EDTA, Hank's Balanced Salt Solution (HBSS), and wheat germ agglutinin (WGA) were purchased from Gibco (Invitrogen Corporation). Transwell® polycarbonate inserts (6 wells, pore diameter of 3 µm polycarbonate, 4.67 cm^2) were purchase from Corning (Madrid, Spain).

2.2. Methods

2.2.1. Preparation and characterization of antioxidant-containing chitosan nanoparticles

Optimized conditions to obtain antioxidant-containing chitosan nanoparticles were previously documented and described [23, 24]. Chitosan nanoparticles were obtained by inducing the gelation of a chitosan solution with TPP. For the study of the best ratio between chitosan:TPP, a volume of the TPP solution of 2 mL was added to 5 mL of the chitosan solution under magnetic stirring at room temperature, thus achieving a final concentration of 2 mg/mL and 0.28 mg/mL of chitosan and TPP, respectively (7:1). The 1% (*w/v*) aqueous rosmarinic acid

and aqueous extracts solutions were added to chitosan previously dissolved in acetic acid at a pH value adjusted to 5.8, in different volumes in order to guarantee the best ratio between chitosan and the different compounds, as previously documented [24]. For this concern, the theoretical encapsulation was fixed in 40% for rosmarinic acid and 50% for sage and savory nanoparticles, fairly to the initial concentration of chitosan (2 mg/mL). Then, nanoparticles were lyophilized (Heto Holten A/S Drywinner) and kept at -20 ºC for 1-2 months

2.2.2. Size and surface charge

Size and polydispersity of freshly unloaded and loaded nanoparticles were determined by photon correlation spectroscopy using ZetaPALS (Brookheaven, New York, USA). A sample of 1.6 mL was gently homogenized, placed into analyzer chamber and measured. Collective 6 readings were performed three times on each sample at 25 ºC with a detection angle of 90º. The zeta potential was determined by laser Doppler anemometry, at 25 ºC. Triplicate samples were also analyzed, each sample being measured 6 times, and the arithmetic mean was adopted.

2.2.3. Association efficiency

Association efficiency (AE) and loading capacity (LC) was evaluated considering the amount of rosmarinic acid associated with the particles. For this purpose the particles were centrifuged (20.000 g for 45 min) and suspended in 7 mL of ultra-pure water. The AE and LC were then calculated by the difference between the total rosmarinic acid used to prepare the particles, and the amount of residual rosmarinic acid in the supernatant. AE and LC of rosmarinic acid in rosmarinic acid nanoparticles, sage and savory nanoparticles were obtained according to the following equation:

$$AE\% = \frac{\text{Total amount of rosmarinic acid} - \text{Free amount of rosmarinic acid in supernatant}}{\text{Total amount of rosmarinic acid}} \times 100$$

$$LC\% = \frac{\text{Total amount of rosmarinic acid} - \text{Free amount of rosmarinic acid in supernatant}}{\text{Rosmarinic acid total weight}} \times 100$$

2.2.4. Mucoadhesion proprieties evaluation by mucin interaction method

An experiment was conducted to determine the chitosan nanoparticles mucoadhesion potential, considering the mucin-particle method. The nanoparticle-mucin interaction was determined measuring the amount of mucin that attaches the nanoparticles, and the success of their connection was evaluated by the variations in size and zeta potential. Particle size, polydispersity and zeta potential of rosmarinic acid-loaded nanoparticles were determined using ZetaPALS (Brookhaven, New York, USA), before and after incubation of nanoparticles in mucin aqueous solution (0.4 mg/mL, incubation conditions: 37 ºC, moderate stirring, for 2 h). Mucin activity was stopped by cooling the particles suspension on ice for 45 min. The conditions applied in this experiment were adapted as previously described [25]. Loaded nanoparticles before incubation with mucin were used as controls. The interaction of mucin in solution with nanoparticles was also assessed by measuring the transmittance of the dispersion, at 372 nm, measured with an UV 1203 spectrophotometer (Shimadzu, Tokyo, Japan), before and after 45 min of incubation time, at three different pH values, namely 5.8, 5.5 and 7.4. This was performed in order to evaluate particle mucin interaction in ionic gelation, ocular inflammation and the homeostasis pH, respectively. Triplicate samples were analyzed, each sample was measured 6 times, and the arithmetic mean value was adopted.

2.2.5. Cell viability and cytotoxicity of nanoparticles

The effect of antioxidant chitosan nanoparticles on cell viability was measured at selected concentrations using the methylthiazolyldiphenyl-tetrazolium bromide conversion (MTT) assay. Cells were seeded in 96-well at 2 x 10^5/well in 0.3 mL with standard medium, consisted of Dulbecco's Modified Eagle Medium (D-MEM) (1X) (Gibco BRL, Grand Island, NY), 10% Fetal Bovine Serum (Heat Inactivated) (Gibco BRL), 0.1 mg/mL streptomycin, and 1000 IU/mL penicillin (both from Gibco BRL) and incubated 24 h at 37 ºC in 5% CO_2 environment. The medium was then changed and the cells were treated with test samples for 4 and 24 h. Each treatment was tested in six individual wells. After time intervals (4 and 24 h), the supernatant was removed and 20 µL of MTT solution (5 mg/mL in HBSS) was added to each well of 96-well plates and then incubated for 2 h at 37°C to allow the formation of formazan crystal. The medium was then removed, and blue formazan was eluted from cells by 150 µL of DMSO. The negative control used, was also DMSO. The plates were shaken on an orbital shaker to solubilize the crystals of formazan. The dark blue crystals were aspirated to another new 96-well plate and measured directly in the plate reader at 570 and 690 nm for background reduction.

The effect of nanoparticles on cell membrane integrity was measured by the lactate dehydrogenase enzyme release (LDH) assays. Ocular cell lines were seeded in 96-well microplates at 2 x 10^5/well and incubated for 24 h at 37 ºC in 5% CO_2 environment. The cultured cells were washed with HBSS (1×) (pre-warmed at 37 ºC). Test solution, and controls (DMEM and DMSO) were added in triplicate to the cell culture. Cells were incubated with medium at 37 ºC for 4 and 24 h. Afterwards, 100 µL of samples were withdrawn and centrifuged for 2 min at 5000 rpm to remove detached cells from the supernatant. The LDH content of 50 µL supernatant was measured at 490 nm (and 690 nm for background deduction) with spectrophotometer using a commercial test kit (Takara, Shiga, Japan) after incubation for 30 min at room temperature in the dark. Cytotoxicity was measured by following the equation:

$$Cytotoxicity\ \% = \frac{Experimental\ value - Low\ control}{High\ control - Low\ control} \times 100$$

249

250 2.2.5.1. Cytotoxicity test using chorioallantoic membrane

251

252 To evaluate the cytotoxicity and biocompatibility of extracts and rosmarinic acid-
253 containing nanoparticles, Hen's Egg Tests (HETs) were performed on the
254 chorioallantoic membrane (CAM) as previously described [26]. HET-CAM test
255 method was used for the detection of ocular corrosives and severe irritants, as
256 defined by the U.S. Environmental Protection Agency (EPA 1996), the
257 European Union (EU; EU 2001), and in the United Nations Globally Harmonized
258 System (GHS) of Classification and Labelling of Chemicals (UN 2003). Fertile
259 hen's eggs at 10 days of incubation at 37 °C, obtained from Guaraves
260 Guarabira Aves Lda, were used in the tests. Five eggs were used for each
261 nanoparticles solution assay. After 10 days of incubation, the egg shell above
262 the air space was removed. The exposed membrane was moistened with a
263 drop of 0.9% physiological saline and the saline was removed, uncovering the
264 chick embryo CAM. An aliquot of 200 µL of nanoparticles solution was applied
265 on the CAM. All assays were repeated five times. Signs of vasoconstriction,
266 hemorrhage and coagulation for 5 min were observed evaluate the potential for
267 irritation according to the method of HET-CAM. The time (in seconds) at which
268 the indicated processes began were applied in Equation [27]. The time (in
269 seconds) at which the indicated processes began were applied in Equation [27]:

270

271 $$Het - Cam\ (IS) = \frac{(301 - h) \times 5}{300} + \frac{(301 - v) \times 7}{300} + \frac{(301 - c) \times 9}{300}$$

272

273 After application of the formula above, it was possible to quantify the observed
274 potential for irritation (irritation score-IS) and to obtain means and standard
275 deviations for the analysis as follows: 0-0.9 no irritation, 1-4.9 slight irritation, 5-
276 8.9 moderate irritation and 9-21 severe irritation [27]. All procedures with
277 chicken eggs were followed by the regulations and procedures for handling of
278 human or animal materials.

2.2.6. Permeability studies

2.2.6.1. Cell monolayers culture

Immortalization of human corneal epithelium (HCE) and retinal pigment epithelium (ARPE) cells have been described earlier. Polycarbonate Transwell® cell culture filters (Corning, 3 µm, 6 wells, USA) were used for permeability assays. Suspension of HCE and ARPE cells were seeded onto the filters at a concentration of 200.000 cells/cm^2. The cells were grown at 37 °C in humidified air with 5% of CO_2, in standard culture medium in apical chamber for 21 to 30 days until the cells were confluent. The culture DMEM medium was replaced every two days.

2.2.6.2. Transepithelial electrical resistance

Transepithelial electrical resistance (TEER) was measured at different phases of cell growth (Evom; World Precision Instruments, Sarasota, FL), as an indicator of epithelial differentiation and epithelial tightness. TEER data were corrected for low-background TEER by using a blank filter containing the possible coating materials and culture medium. At the end of each permeability experiment, TEER was measured to detect the condition of the cells.

2.2.6.3. Permeation studies in cell monolayers

The permeation study with different solutions was initiated by washing with HBSS (1x) liquid (without calcium and magnesium) both the basolateral and apical side one time and then adding 2.5 mL of HBSS to the basolateral side (receiver side) and 1.5 mL of HBSS to the apical side (donor side). At different

time points, during 60 minutes, aliquots of 100 µL were withdrawn from the receiver chamber and replaced with an equal volume of blank medium. TEER was measure at each time and the plates were incubated with the sample at 37 ºC to sum to the test times. P_{app} was calculated from the measurement of the flow rate of insulin from the donor to the acceptor chambers:

$$Papp\ (cm/s) = dQ/dt\ (A \times C0)$$

where, dQ is the total amount of permeated rosmarinic acid (mg), A is the diffusion area (cm^2), C0 is the initial concentration of rosmarinic acid (mg/mL), and dt is the time of experiment in seconds (s). The coefficient dQ/dt represents the steady-state flux of rosmarinic acid across the monolayer.

2.2.6.4. High performance liquid chromatography analysis

The HPLC method was developed and validated, as previously described [24]. Briefly, aliquots of 100 µL were injected at HPLC to quantify which quantity concentration permeates to the basolateral side of the plates. All HPLC runs were performed using a Waters Series 600 HPLC and results were acquired and processed with Empower® Software 2002 for data acquisition (Mildford MA, USA). HPLC analysis was conducted by using a Nova-Pack® RP C18 column (250 x 4.6 mm i.d., 5 µm particle size and 125 Å pore size) from Waters. Chromatographic analysis was performed in gradient mode. The mobile phase consisted of methanol: formic acid: water UP in the ratio 92.5:2.5:5 (*v/v*). Stationary phase was made with the same components in the ratio of 5:2.5:92.5, respectively. The phases were filtrated through 0.22 µm filter and degassed. Eluent was pumped at a flow rate of 0.75 mL/min, the injection volume was 20 µL and detection wavelength was 280 nm.

2.2.7. Statistical analysis

Statistical analysis was performed using IBM SPSS Statistics v 19.0.0 (Illinois, USA). The one-way analysis of variance (ANOVA) was used with Scheffé post hoc test comparison of groups with normal distribution, and Mann-Whitney test for groups with non-normal distribution. Differences were considered to be significant at a level of $P < 0.05$.

3. Results and discussion

3.1.1. Particle size, polydispersity and zeta potential

The particle size and mean size distribution are fundamental features that influence the *in vivo* distribution, biological fate, toxicity and the targeting ability of nanoparticles containing therapeutic drugs [28]. It is also known that the highest value of zeta potential represents the greater electrostatic repulsive interactions among the particles. Zeta potential values of ± 30 mV indicates that the colloidal systems are stable in time and that amine groups of chitosan are on the surface [29]. The developed nanoparticles ranged from 200-300 nm in size and zeta potential were around 20-30 mV (Table 1). It is described that for ultrafine particles the induction of reactive oxygen species, oxidative stress, inflammation and vasculature are a risk [30]. In this sense it can be considered that the particles of this study will have no such harmful effects. Moreover, the results are in agreement with similar nanoparticles containing rosmarinic acid recently developed [31] and with other extracts, also encapsulated in chitosan nanoparticles [29]. The results did not show significant differences ($P > 0.05$) in size between the rosmarinic acid and the two crude extracts, as previously described [23, 24]. This may be due to the high rosmarinic acid content in extracts composition 10 and 5% in sage and savory, respectively [23]. Thus the extracts under study are promising vehicles for rosmarinic acid nano-incorporation, as previously documented [23, 24]. The size obtained is also in agreement with ocular drug delivery demands, as particles with size ≤ 200 nm were observed to reach the retina, vitreous and trabecular meshwork [32] and have more vitreal half-life compared to huge nanoparticles [33]. The obtained nanoparticles also showed values of polydispersity between 0.1 and 0.2

corresponding to a narrow distribution and monodispersed particles. These results are in accordance to other works using similar antioxidant nanoparticles [34].

Table 1. Insertion here

3.1.2. Association efficiency and loading capacity

Chitosan can interact with the negatively charged TPP, forming inter- and intra-molecular cross-linkages, yielding ionically cross-linked chitosan nanoparticles in acidic media (pKa 6.5) [35]. It is also known that the inter- and intra-molecular linkages created between TPP and the positively charged amine groups of chitosan were responsible for the success of the gelation process [36]. Among the different sources of rosmarinic acid encapsulated into chitosan nanoparticles, it was observed different loading capacity between free drug and extracts (Table 1). This may be correlated to the lower initial amount in rosmarinic acid used to prepare nanocomplexes, as previously described for insulin encapsulation into chitosan-alginate ionotropic nanoparticles [37]. The results were in line with previous data for ionic gelation chitosan nanoparticles [38, 39]. Higher association efficiency was found for rosmarinic acid entrapment in extracts of sage and savory (with no significant differences observed between them ($P > 0.05$), than in pure rosmarinic acid entrapment in chitosan nanoparticles. The results were on the row with other chitosan idebenone and *ilex paraguensis* encapsulation [29, 40]. Other studies showed similar association efficiency for other phenolic compound, such as cathechin [41] and epigallocatechin gallate [42]. The results also exhibited higher association efficiency than the obtained for quercetin encapsulation in polylactic acid (PLA) nanoparticles (i.e. 40%) [43]. Nevertheless, higher association efficiency for rosmarinic acid nanoparticles were previous described in solid-lipid-nanoparticles [31]. Nevertheless, higher association efficiency for rosmarinic acid nanoparticles were previous described in solid-lipid-nanoparticles [31].

Therefore, the association efficiency was highly dependent on the nanosystem used, as well as from the loading and rosmarinic acid amount utilized into the nanoparticles.

3.1.3. Mucoadhesion proprieties evaluation by mucin interaction method

Ocular mucosa may affect the stability chitosan nanoparticles in the presence of mucus components [44]. Mucus consists in a heterogeneous tridimensional network, being basically composed of a mucin fibers network, creating an endless system of canals in which particles can diffuse and/or be retained [45, 46]. Chitosan is a mucoadhesive polymer that may increase residence time and intimate contact of the delivery vehicle with the mucosa, consequently increasing the drug bioavailability, such proprieties were well documented in literature [47]. The chitosan adhesion mechanism is mainly associated to the electrostatic interactions established between protonated amine groups of mucoadhesive chitosan and negatively charged groups of mucin [48]. In this study, the nanoparticle-mucin interaction was determined measuring the amount of mucin that attaches the nanoparticles [49]. The degree of adsorption of nanoparticles/mucin particles can be determined by the variations in size [50], zeta potential [51] or electrophoretic mobility [52] of formed complexes with mucosal fluids, in particular with mucin. Size can influence the diffusion of drug carriers through the mucin mesh that composes mucus fluids, being the optimal range between 200 and 500 nm to enhance diffusion [53]. Higher or smaller diameters may decrease transport through the mucus layer. This is in contrast to the prevailing belief, demonstrate that large nanoparticles, can rapidly penetrate physiological human mucus, and that large nanoparticles can be used for mucosal drug delivery [53]. For this purpose, rosmarinic acid containing nanoparticles were evaluated, since chitosan was the only responsible for the mucoadhesion results and rosmarinic acid was the principle active of all the formulations used. As depicted in Table 2, the rosmarinic acid nanoparticles obtained in this study were in optimal range mentioned, for the three pHs used. The influence of pH values was intended to demonstrate that the particles were

mucoadhesive in different conditions, at the normal ionic gelation pH (5.8), at an inflammation pH (5.0) and in homeostasis pH (7.4). The increased size after mucin incubation suggests that nanoparticles-mucin interaction were forming microaggregates, and decrease in zeta potential values was probably due to the electrostatic interaction between positive charged of chitosan and anionic mucin [51]. Strong ability of those nanoparticles to interact with mucin through electrostatic forces were observed, highlighting their potential as mucoadhesive carriers [25]. Other study demonstrated the effect of low, medium and high molar mass chitosan in coated poly-caprolactone (PCL) nanoparticles [48]. The results were according to mucoadhesive nanoparticles made of thiolated quaternary chitosan crosslinked with hyaluronan [54].

Table 2. Insertion here

3.1.4. Cell viability studies

In order to evaluate any potential cytotoxicity of rosmarinic acid, sage and savory on ARPE-19 and HCE-T cell lines, pure rosmarinic acid and extracts-loaded chitosan nanoparticles were tested for 4 and 24 h. The effect of nanoparticles on membrane integrity was measured by the LDH enzyme release assay and the effect on cell viability was measured using the MTT conversion assay. *In vitro* cytotoxicity results were presented in (Figure 1). Results showed that after 4 h the cytotoxicity was below 10% for the tested concentration range, for both cells lines. Moreover, there were no significant differences ($P > 0.05$) between the 4 and 24 h (testing time) considering all

Figure 1. Insertion here

Results of cell viability for rosmarinic acid, sage and savory loaded chitosan nanoparticles obtained from the MTT test were shown in Figure 2. These were

in a good correlation with those from the LDH assay. Antioxidant/chitosan nanoparticles presented a good profile in terms of cell viability of ARPE-19 and HCE-T cells. The results showed that these nanoparticles were not toxic for the cells at concentrations below 1 mg/mL. The results were in line with chitosan cell safety performance regarding its use as drug delivery systems and data show that it was completely safe with no-toxicity effect upon cell lines since chitosan can interact with cell membranes and be uptake with no cytotoxicity and cell collateral damages. The results were in line with previous studies on the use of chitosan in drug delivery systems, [55] regarding its non-toxicity, good cell membrane interaction and cellular uptake with no collateral damages. Moreover, other studies demonstrated that chitosan nanoparticles besides being non-toxic, may have protective effects on cell lines [56-58].

Figure 2. Insertion here

The cellular models have been established as promising tools for the investigation of pathological ocular conditions, and the toxicological screening of compounds as alternative to *in vivo* toxicity tests. Animal based experiments are important for pharmacological and toxicological studies while cell models are relevant to mechanistic researches [59]. Several animal models including rabbits, pigs, rats and monkeys have been exploited for studies of ocular drug pharmacokinetics and bioavailability. The ethical controversy associated to these biological trials implies the need to develop cell cultures that mimic the action of drugs on the organism. It is now known that the development and validation of *in vitro* tests to replace animal experimentation is among the priorities of the 7th European Community framework program [59, 60]. Several studies have been conducted to evaluate the feasibility of using HET-CAM as a complete replacement for the *in vivo* rabbit ocular test (Draize test). This test has several advantages, such as avoiding the ethical concerns, allow high simplicity, rapid, sensitive and easily performance. It is also an economic method to simulate *in vivo* ocular reactions [61]. Animal experiments regulation allows protocols that use chick embryos without needing authorization from

494 animal experimentation committees [61]. The HET-CAM test has been
495 proposed as a model for a living membrane because it has a functional
496 vasculature, in other words, the acute effects induced by a test substance on
497 the small blood vessels and proteins of this soft tissue membrane are similar to
498 those of the rabbit eye test, while offering the advantages of being a non-animal
499 test, more rapidly and universally acceptable. For that reason, HET-CAM
500 cytotoxicity test was intended to evaluate the development of irritation
501 symptoms. Cytotoxicity of rosmarinic acid, sage and savory-loaded chitosan
502 nanoparticles was then evaluated for hemorrhage, coagulation (intra- and
503 extravascular protein denaturation) and vasoconstriction, when the test
504 substances were added to the membrane and left in contact for 5 min (Table 3).
505 The particles were shown to be non-irritating (IS = 0.0) because they did not
506 prompt vasoconstriction, haemorrhage or coagulation in the HET-CAM cells
507 within 5 min of contact. These results were in agreement with the MTT and LDH
508 assays made before, and with those obtained elsewhere for chitosan, chitosan
509 nanoparticles and other nanosystems [26, 62-64].

510

511 **Table 3. Insertion here**

512

513 ### 3.1.5. Permeability assays

514

515 Only about 1-5% of a topically applied drug dose often reaches the anterior
516 segment of the eye [65]. Therefore, the subsequent diffusion of drugs to the
517 posterior segment will often be low. Moreover eye drops in solution are
518 eliminated from the precorneal area within 90 seconds and absorbed
519 systemically through the highly vascular conjunctival stroma and nasolachrymal
520 ducts [66]. This means that drugs topically administered have low probability of
521 reaching the posterior segment in significant amounts (due to corneal and
522 conjunctival epithelium, then aqueous humor, and lens physical barriers) [67].
523 Undoubtedly, the permeation of a molecule is determined by the delicate
524 balance of numerous parameters that are clearly interrelated. In modern
525 pharmacological discovery stage, the study of biological activity and drug

physical-chemical profile are crucial. Some of these core properties are the aqueous solubility, lipophilicity and membrane permeability, which will influence the transport, cellular uptake and distribution of chemicals in biological systems [68].

In the ocular system, the drug absorption from the surface of the eye can be summarized in either corneal or noncorneal [69]. Mostly drugs are passive diffused across the cornea and this diffusion transport is influenced by solubility, molecular weight, partition coefficient and drug ionization degree [68]. In structure, the corneal epithelium is the main limiting barrier for hydrophilic drugs that penetrate through the paracellular pathway, but in another way, hydrophilic compounds may have the diffusion eased in cornea hydrophilic stroma, which also is the most tightness structure of cornea and represents 85-90% of cornea total mass [60]. In the opposite case, the lipophilic compounds are able to permeate through the cornea epithelium via transcellular route, nonetheless, they will deal with a huge difficulty to cross the stroma [65]. Having this in mind, chitosan mucoadhesive carriers that increases the retention time in ocular surface may be, in the future, a crucial solution in topical administration.

In this study, after morphological characterization, mucoadhesion, and viability assays, the rosmarinic acid transport study was conducted to track the effect of chitosan nanoparticles on the *in vitro* permeability. The transport of rosmarinic acid (loaded chitosan-based nanoparticles and free in solution) was tracked through the different ocular cell models (e.g. ARPE and HCE), following by the measurement of rosmarinic acid transport across the cells. For these permeability experiments, initial TEER values were ≈ 300 Ωcm^2, for both cell lines, at 21 days of post-seeding (90-100% confluence) on the Transwell®. The results demonstrated similar P_{app} after 1 h, for both rosmarinic acid (loaded chitosan-based nanoparticles and free in solution) and for both cell lines, with no significant differences ($P > 0.05$) between wither loaded and free solution or cells. HCE cell line permeability study showed a P_{app} of $3.41 \pm 0.99 \times 10^{-5}$ and $3.24 \pm 0.79 \times 10^{-5}$ cm/s for rosmarinic acid loaded chitosan-based nanoparticles and free in solution, respectively (Figure 3). In ARPE-19 cell study the P_{app} was $3.39 \pm 0.18 \times 10^{-5}$ and $3.60 \pm 0.05 \times 10^{-5}$ cm/s for rosmarinic acid loaded chitosan-based nanoparticles and free in solution, respectively (Figure 4). P_{app} was calculated considering only the apical to basolateral direction. No

significant differences between formulations neither between cell lines (P > 0.05) were observed. Regarding TEER results it has been reported ARPE-19 TEER values of 30, 100 and higher than 200 Ωcm^2 [20]. Thus, the great disparity in the TEER values found in the literature was probably due to differences in post seeding time and percentage of confluence of ARPE-19 cell lines. Regarding the HCE-T cell line, TEER values obtained were expectable and similar to those reported by Nagai et al. (ca. 400 Ωcm^2). The TEER values under studied guarantee that the established monolayers were considered to be tight enough for permeability experiments [60]. In the same way as TEER values, P_{app} values can also depend on various factors such as passage number, age of the cells, the media and growth conditions used and even the own TEER values [70]. For this reason, this technique was more precise when a comparative manner with all the compounds assessed in the same assay and under the same conditions. The P_{app} values may allow the permeability compounds rating into poorly, moderately, and highly permeable (P_{app} < 1 x 10^{-6}, 1-10 x 10^{-6}, and >10 x 10^{-6} cm/s, respectively) [71, 72]. Considering this, and the rosmarinic acid P_{app} values (>10 x 10^{-6} cm/s) it can be predicted that this phenolic acid was highly permeable in ocular cell lines. In fact, the low molecular weight (i.e. 360.31) of this compound was in the range of "non-restricted membrane diffusion" [73]. Also, its hydrophilic character and consequent passive diffusion trough the paracellular route was predictable. The increase of rosmarinic acid permeability during the time in HCE-T and ARPE-19 cell lines was deeply related with the decrease of tight junction stickiness, tracked by the deacrease of TEER values found for the cell culture during the time of the experiment, promoting the paracelular transport of rosmarinic acid (Figure 3 and 4). It is already known that as the tight junctions open, the TEER values of cell monolayers are significantly reduced, due to ion passages through the paracellular route [74]. It was expectable that chitosan enhanced rosmarinic acid cell permeability, due to its ability to open epithelium tight junctions. In addition, the chitosan is also commonly explored for improving precorneal residence of nanoparticles because it is positively charged which hence it binding to negatively charged corneal surface and thereby improves precorneal residence and decreases clearance [75]. Nevertheless, chitosan permeation effect was not observed in this study, since no significant

differences were detected in permeation between rosmarinic acid loaded chitosan nanoparticles or free in solution. One important fact that may be on the base of the absence of enhancement effect of chitosan nanoparticles was the natural rapid release profile of these particles described previously [23, 24]. Since that in the first 15-20 min over 50 to 60% was released at physiological pH, which was the ideal profile when it is not needed to prolong the drug release for several hours, as in the case of ophthalmic solutions. This may be one of the reasons that from this time on, no significant differences could be found between nanoformulation and the free compound. These solutions must ensure the best compromise between efficiency and minimum residence time possible in order to not cause discomfort to the patient. The permeability values were higher than other previous reports considering rosmarinic acid in *Prunella vulgaris* and ursolic acid in *Salvia officinalis* extracts across Caco-2 cell monolayers [76]. Moreover, the results were also in the line with those reported in other study, which showed rosmarinic acid intestinal absorption efficiency and evidences of transport mainly via paracelluar diffusion [77]. Furthermore, it was described that rosmarinic acid appeared to be unsusceptible to hydrolysis by mucosa esterase in Caco-2 cells and further metabolized and degraded into m-coumaric and hydroxylated phenylpropionic acids by gut microflora, which were then efficiently absorbed and distributed by the monocarboxylic acid transporter (MCT) within the body [77]. Notwithstanding and besides no enhancement permeability effect was observed in chitosan encapsulation of rosmarinic acid, it should be underline the chitosan mucoadhesiveness proprieties that are crucial to overcome the drug lost by blinking process that happens in the first 90 s [66]. In this sense it is vital the particles adherence and protection of the drug delivery in the first brief minutes, as chitosan particles ensure in this study.

Figure 3. Insertion here

Figure 4. Insertion here

4. Conclusion

In this study, was reported an extensive *in vitro* study for chitosan nanoparticles encapsulating rosmarinic acid, in a pure form, and also in two different natural extracts (e.g. sage and savory). Results demonstrated mucoadhesive nanoparticles ranging 200-300 nm with a surface charge between 20-30 mV and without relevant cytotoxicity against ocular cell lines (e.g. ARPE and HCE). Rosmarinic acid showed to be a compound highly permeable (loaded and unloaded chitosan nanoparticles), regarding both studied cell lines above (3.2 x 10^{-5} cm/s) after 60 min. In this study it was proposed, for the first time, chitosan formulations as biodegradable mucoadhesive nanocarriers for delivery of rosmarinic acid, sage and savory natural antioxidants that in newer future may represent a suitable alternative to current invasive clinical methods. Nonetheless a better correlation with *in vivo* data should be deeply explored, in order to understand the real potential of these systems in ocular diseases prevention and treatment.

5. Acknowledgements

Funding for author Sara B. Silva was via a PhD fellowship, administered by Fundação para a Ciência e a Tecnologia (SFRH/BD/61423/2009). This work was supported by National Funds from FCT – Fundação para a Ciência e a Tecnologia through project PEst-OE/EQB/LA0016/2013.

This work was also financed by European Regional Development Fund (ERDF) through the Programa Operacional Factores de Competitividade – COMPETE, by Portuguese funds through FCT – Fundação para a Ciência e a Tecnologia in the framework of the project PEst-OE/EQB/LA0016/2013, and co-financed by North Portugal Regional Operational Programme (ON.2 – O Novo Norte) in the framework of project SAESCTN-PIIC&DT/2011, under the National Strategic Reference Framework (NSRF).

6. References

[1] M. de la Fuente, M. Raviña, P. Paolicelli, A. Sanchez, B. Seijo, M.J. Alonso, Adv. Drug Delivery Rev., 62 (2010) 100-117.

[2] S.K. Sahoo, F. Dilnawaz, S. Krishnakumar, Drug Discov. Today, 13 (2008) 144-151.

[3] Y.C. Kim, B. Chiang, X. Wu, M.R. Prausnitz, J. Control. Release, 190 (2014) 172-181.

[4] A. Sosnik, J. das Neves, B. Sarmento, Prog. Polym. Sci., In press (2014).

[5] S.B.d. Silva, S. Borges, Ó. Ramos, M. Pintado, D. Ferreira, B. Sarmento, Treating retinopathies: Nanotechnology as a tool in protecting antioxidants agents, in: Syst. Biol. Free Radical Antiox., Springer-Verlag, Germany, 2014.

[6] B.R. Hammond, B. Johnson, E.R. George, Exp. Eye Res., In press (2014).

[7] H. Lee, H. Arnouk, S. Sripathi, P. Chen, R. Zhang, M. Bartoli, R.C. Hunt, W.J.M. Hrushesky, H. Chung, S.H. Lee, W.J. Jahng, Int. J. Biol. Macromol., 47 (2010) 685-690.

[8] R.A. Kowluru, P. Koppolu, Free Radical Res., 36 (2002) 993–999.

[9] A.S. Andrade, T.B. Salomon, C.S. Behling, C.D. Mahl, F.S. Hackenhaar, J. Putti, M.S. Benfato, Exp. Eye Res., 120 (2014) 1-9.

[10] A.V. Saijyothi, J. Fowjana, S. Madhumathi, M. Rajeshwari, M. Thennarasu, P. Prema, N. Angayarkanni, Exp. Eye Res., 103 (2012) 41-46.

[11] M. Petersena, M.S.J. Simmonds, Phytochemistry, 62 (2003) 121–125.

[12] F. Shahidi, P.K. Yanita, P.D. Nanosudra, Crit. Rev. Food Sci., 32 (1992) 67-103.

[13] M.S. Gião, C.I. Pereira, S.C. Fonseca, M.E. Pintado, F.X. Malcata, Food Chemistry, 117 (2009) 412-416

[14] R.A. Kowluru, P.-S. Chan, Exp. Diabetes Res., 2007 (2007) 1-12.

[15] R.N. Frank, Am. J. Ophtalmol., 133 (2002) 693-698.

[16] K. Kalishwaralal, S. BarathManiKanth, S. Ram, K. Pandian, V. Deepak, S. Gurunathan, J. Control. Release, 145 (2010) 2.

[17] D.V. Ratnam, D.D. Ankola, V. Bhardwaj, D.K. Sahana, M.N.V. Ravi Kumar, J. Control. Release, 113 (2006) 189–207.

[18] A.S. Guinedi, N.D. Mortada, S. Mansour, R.M. Hathout, Int. J. Pharm., 306 (2005) 71-82.

[19] R.S. Bhatta, H. Chandasana, Y.S. Chhonker, C. Rathi, D. Kumar, K. Mitra, P.K. Shukla, Int. J. Pharm., 432 (2012) 105-112.

[20] E. Mannermaa, M. Reinisalo, V.-P. Ranta, K.-S. Vellonen, H. Kokki, A. Saarikko, K. Kaarniranta, A. Urtti, Eur. J. Pharm. Sci., 40 (2010) 289–296.

[21] E. Toropainen, V.-P. Ranta, K.-S. Vellonen, J. Palmgrén, A. Talvitie, M. Laavola, P. Suhonen, K.M. Hämäläinen, S. Auriola, A. Urtti, Eur. J. Pharm. Sci., 20 (2003) 99-106.

[22] M. Garcia-Ramírez, C. Hernández, M. Ruiz-Meana, M. Villarroel, L. Corraliza, D. García-Dorado, R. Simó, Cell. Signal., 23 (2011) 1596-1602.

[23] S.B.d. Silva, M. Amorim, P. Fonte, R. Madureira, D. Ferreira, M. Pintado, B. Sarmento, Pharm. Biol., In press (2014).

[24] S.B.d. Silva, A. Oliveira, D. Ferreira, B. Sarmento, M. Pintado, Phytochem. Anal., 24 (2013) 638-644.

[25] L. Mazzarino, C. Travelet, S. Ortega-Murillo, I. Otsuka, I. Pignot-Paintrand, E. Lemos-Senna, R. Borsali, J. Colloid Interface Sci., 370 (2012) 58–66.

[26] L. Berger, T. Stamford, T. Stamford-Arnaud, L. Franco, A. Nascimento, H. Cavalcante, R. Macedo, G. Campos-Takaki, Molecules, 19 (2014) 2771-2792.

[27] S. Kalweit, R. Besoke, I. Gerner, H. Spielmann, Toxicology *In Vitro*, 4 (1990) 702–706.

[28] A. Kumari, S. Yadav, Y. Pakade, B. Singh, S. Yadav, Colloids Surf. B, 80 (2010) 184-192.

[29] R. Harris, E. Lecumberri, I. Mateos-Aparicio, M. Mengíbar, A. Heras, Carbohydr. Polym., 84 (2011) 803-806.

[30] T. Xia, M. Kovochich, J. Brant, M. Hotze, J. Sempf, T. Oberley, C. Sioutas, J.I. Yeh, M.R. Wiesner, A.E. Nel, Nano Lett., 6 (2006) 1794-1807.

[31] D.A. Campos, A.R. Madureira, A.M. Gomes, B. Sarmento, M.M. Pintado, Colloids Surf. B, 115 (2014) 109-117.

[32] E. Sakurai, H. Ozeki, N. Kunou, Y. Ogura, Ophthalmic Res., 33 (2001) 31-36.

[33] U.B. Kompella, A.C. Amrite, R.P. Ravi, S.A. Durazo, Prog. Retin. Eye Res., 36 (2013) 172-198.

[34] Y. Liu, Y. Sun, Y. Li, S. Xu, J. Tang, J. Ding, Y. Xu, Carbohydr. Polym., 83 (2011) 1162-1168.

[35] M.J. Alonso, A. Sanchéz, J. Pharm. Pharmacol., 55 (2003) 1451-1463.

[36] P. Calvo, C. Remunan-Lopez, J.L. Vila-Jato, M.J. Alonso, J. Appl. Polym. Sci., 63 (1997) 125-132.

[37] B. Sarmento, S. Martins, A. Ribeiro, F. Veiga, R. Neufeld, D. Ferreira, Int. J. Pept. Res. Ther., 12 (2006) 131-138.

[38] S.F. Hosseini, M. Zandi, M. Rezaei, F. Farahmandghavi, Carbohydr. Polym., 95 (2013) 50-56.

[39] M.A. Azevedo, A.I. Bourbon, A.A. Vicente, M.A. Cerqueira, Int. J. Biol. Macromol., In press (2014).

[40] C. Amorim, A. Couto, D. Netz, R. Freitas, T. Bresolin, Nanomed. Nanotech. Biol. Med., 6 (2010) 745-752.

[41] A.R. Dudhania, S.L. Kosarajua, Carbohydr. Polym., 81 (2010) 243-251.

[42] I. Peres, S. Rocha, J. Gomes, S. Morais, C. Pereira, M. Coelho, Carbohydr. Polym., 86 (2011) 147-153.

[43] A. Kumari, SudeshYadav, Y. Pakade, V. Kumar, B. Singh, A. Chaudhary, S. Yadav, Colloids Surf. B, 82 (2011) 224-232.

[44] A. Campos, Y. Diebold, E. Carvalho, A. Sánchez, M.J. Alonso, Pharm. Res., 21 (2004) 803-810.

[45] S.S. Olmsted, J.L. Padgett, A.I. Yudin, K.J. Whaley, T.R. Moench, R.A. Cone, Biophys. J., 81 (2001) 1930-1937.

[46] J.d. Neves, M.F. Bahia, M.M. Amiji, B. Sarmento, Expet. Opin. Drug Deliv., 8 (2011) 1085-1104.

[47] K. Leithner, A. Bernkop-Schnürch, Chitosan and Derivatives for Biopharmaceutical Use: Mucoadhesive Properties in: B. Sarmento, J.d. Neves (Eds.) Chitosan-Based Systems for Biopharmaceuticals: Delivery, Targeting and Polymer, John Wiley & Sons, Ltd, 2012, pp. 159-180.

[48] L. Mazzarino, L. Coche-Guérente, P. Labbé, E. Lemos-Senna, R. Borsali, J. Biom. Nanotechnol., 9 (2013) 1-8.

[49] H. Takeuchi, J. Thongborisute, Y. Matsui, H. Sugihara, H. Yamamoto, Y. Kawashima, Adv. Drug Delivery Rev., 57 (2005) 1583-1594.
[50] C. Mugabe, B.A. Hadaschik, R.K. Kainthan, D.E. Brooks, A.I. So, M.E. Gleave, H.M. Burt, British Journal of Urology International, 103 (2009) 978-986.
[51] A. Jintapattanakit, V.B. Junyaprasert, T. Kissel, J. Pharm. Sci., 98 (2009) 4818-4830.
[52] O. Svensson, K. Thuresson, T. Arnebrant, Langmuir, 24 (2008) 2573-2579.
[53] S. Lai, E. O'Hanlon, J. Hanes, Proc. Natl. Acad. Sci. U. S. A., 104 (2007) 1482-1487.
[54] Y. Zambito, F. Felice, A. Fabiano, R.D. Stefano, G.D. Colo, Carbohydr. Polym., 92 (2013) 33–39.
[55] F. Andrade, F. Antunes, A.V. Nascimento, S.B.d. Silva, J.d. Neves, D. Ferreira, B. Sarmento, Curr. Drug Discov, Technol,, 8 (2011) 157-172.
[56] Z.-S. Wen, L.-J. Liu, Y.-L. Qu, X.-K. OuYang, L.-Y. Yang, Z.-R. Xu, Mar. Drugs, 11 (2013) 3582-3600.
[57] D. Narayanan, A. Anitha, R. Jayakumar, S.V. Nair, K.P. Chennazhi, J. Biom. Nanotechnol., 8 (2012) 98-106.
[58] H. Ragelle, R. Riva, V. G., B. Naeye, V. Pourcelle, C.S. Le Duff, C. D'Haese, B. Nysten, K. Braeckmans, S.C. De Smedt, C. Jérôme, V. Préat, J. Control. Release, 176 (2014) 54–63.
[59] J. Barar, M. Asadi, S. Abdolreza, Mortazavi-Tabatabaei, Y. Omidi, J. Ophthalmol. Vis. Res., 4 (2009) 238-252.
[60] M. Hornof, E. Toropainen, A. Urtti, Europ. J. Pharm. Biopharmac., 60 (2005) 207-225.
[61] A. Vargas, M. Zeisser-Labouèbe, N. Lange, R. Gurny, F. Delie, Adv. Drug Delivery Rev., 59 (2007) 1162–1176.
[62] L. Rahul, A. Verma, S. Jain, Int. J. Pharm. Sci., 1 (2012) 732 -737.
[63] U. Shinde, M.H. Ahmed, K. Singh, J. Drug Deliv., 2013 (2013) 562-727.
[64] G. Himanshu, M. Aqil, R.K. Khar, A. Ali, A. Bhatnagar, G. Mittal, J. Drug Target., 19 (2011) 409–417.
[65] S.B.d. Silva, J.P. Costa, M.E. Pintado, D.d.C. Ferreira, B. Sarmento, J. Diabetes Metabol., 1 (2010).

785 [66] H.J. Gukasyan, K.-J. Kim, V.H.L. Lee, The Conjunctival Barrier in Ocular
786 Drug Delivery, in: C. Ehrhardt, K.J. Kim (Eds.) Drug Absorption Studies: *In Situ*,
787 *In Vitro* and *In Silico*, Springer, New York, 2008, pp. 307-320.
788 [67] S. Gunda, S. Hariharan, N. Mandava, A.K. Mitra, Barriers in Ocular Drug
789 Delivery, in: J.T.-T.a.C.J. Barnstable (Ed.) Ophthalmology Research: Ocular
790 Transporters in Ophthalmic Diseases and Drug Delivery, Human Press, 2008,
791 pp. 399-413.
792 [68] C. Hernández-Covarrubias, M.A. Vilchis-Reyes, L. Yépez-Mulia, R.
793 Sánchez-Díaz, G. Navarrete-Vázquez, A. Hernández-Campos, R. Castillo, F.
794 Hernández-Luis, Eur. J. Med. Chem., 52 (2012) 193-204.
795 [69] D. Ghate, H.F. Edelhauser, Expert Opinion on Drug Delivery, 3 (2006) 275-
796 287.
797 [70] I. Behrens, W. Kamm, A.H. Dantzig, T. Kissel, J. Pharm. Sci., 93 (2004)
798 1743-1754.
799 [71] M.I. Kaldas, U.K. Walle, T. Walle, J. Pharm. Pharmacol., 55 (2003) 307-
800 312.
801 [72] T. Fichert, M. Yazdanian, J.R. Proudfoot, Bioorg. Med. Chem. Lett., 13
802 (2003) 719-722.
803 [73] G. Camenisch, J. Alsenz, H. van de Waterbeemd, G. Folkers, Eur. J.
804 Pharm. Sci., 6 (1998) 317-324.
805 [74] Z. Yildirim, N. Irem Ucgun, N. Kilic, G. E., A. Sepici-Dinçel, Ann. N. Y.
806 Acad. Sci., 1100 (2007) 199–206.
807 [75] A. Patel, K. Cholkar, V. Agrahari, A.K. Mitra, World J. Pharmacol., 9 (2013)
808 47-64.
809 [76] Z. Qiang, Z. Ye, C. Hauck, P. Murphy, J.-A. McCoy, M. Widrlechner, M.
810 Reddy, S. Hendrich, J. Ethnopharmacol., 137 (2011) 1107– 1112.
811 [77] Y. Konishi, S. Kobayashi, Biosci. Biotechnol. Biochem., 69 (2005) 583-591.

812

813 **Captions**

814

Table 1. Average hydrodynamic diameter (*Z*), polydispersity index (*PdI*) and zeta potential of chitosan nanoparticles loaded rosmarinic acid, sage and savory.

Nano	*Z*-average (nm)	*PdI*	Zeta potential (mV)	Association efficiency (%)	Loading capacity (%)
RA	280.0 ± 16.0 ^{a}	0.201 ± 0.091 ^{b}	30.1 ± 1.8 ^{c}	60.2 ± 1.3 ^{d}	5.3 ± 0.4 ^{f}
Sage	302.4 ± 18.2 ^{a}	0.288 ± 0.074 ^{b}	27.5 ± 0.9 ^{c}	96.8 ± 0.2 ^{e}	8.1 ± 0.6 ^{g}
Savory	298.3 ± 20.8 ^{a}	0.214 ± 0.085 ^{b}	28.2 ± 2.2 ^{c}	98.0 ± 0.3 ^{e}	7.8 ± 0.2 ^{g}

Note: Values were means of triplicate samples ± standard deviation; ^{a,b,c,d,e,f,g} means within the same column, labelled with the same letter, were not statistically different from each other ($P > 0.05$).

Table 2. Average hydrodynamic diameter (*Z*), polydispersity index (*PdI*) and zeta potential of chitosan nanoparticles loaded rosmarinic acid before and after mucin interaction (n = 3).

Nanoparticles	pH	*Z*-average (nm)	*PdI*	Zeta potential (mV)
Rosmarinic acid	5.8	236.0 ± 7.1^{a}	0.719 ± 0.036	40.1 ± 0.8 ^{c}
Rosmarinic acid + Mucin	5.0	488.2 ± 30.5 ^{b}	0.619 ± 0.049	22.5 ± 0.9 ^{d}
Rosmarinic acid + Mucin	7.4	414.1 ± 32.3 ^{b}	0.511 ± 0.014	23.1 ± 0.6 ^{d}

Note: Values were means of triplicate samples ± standard deviation; [a, b, c, d] means within the same column, labelled with the same letter, were not statistically different from each other ($P > 0.05$).

Table 3. Cytotoxicity of rosmarinic acid, sage and savory-loaded chitosan nanoparticles for development of irritation symptoms such as vasoconstriction, hemorrhage and coagulation.

	Nanoparticles			
Assays	Sage	Savory	Rosmarinic acid	SLS 1%
Vasoconstriction	n. o.	n. o.	n. o.	7 ± 0.6
Hemorrhage	n. o.	n. o.	n. o.	49 ± 2.0
Coagulation	n. o.	n. o.	n. o.	68 ± 3.0
Irritation Potential	0.0 ± 0.0	0.0 ± 0.0	0.0 ± 0.0	18 ± 0.5

Note: Positive control - sodium lauryl sulfate 1% (SLS). n.o. signs not observed. Non-irritating: 0-0.9; slightly irritating: 1-4.9; Irritating: 5-8.9 and severely irritating: 9-21.

Figure 1. Effect of rosmarinic acid, sage and savory-loaded chitosan nanoparticles on cell cytotoxicity of ARPE (A, C and E) and HCE (B, D and F) cell lines after 4 h (black bar) and 24 h (white bar) of incubation. DMEM+cells and DMSO were used as controls. The formulation concentration used was displayed in the tables, relatively to rosmarinic acid (A, B), sage (C, D) and savory (E, F) (results were the mean of 6 replicates, bars represent standard deviation).

Figure 2. Effect of rosmarinic acid, sage and savory-loaded chitosan nanoparticles on viability of ARPE (A, C and E) and HCE (B, D and F) cell lines after 4 h (black bar) and 24 h (white bar) of incubation. DMEM+cells and DMSO were used as controls. The formulation concentration used was displayed in the tables, relatively to rosmarinic acid (A, B), sage (C, D) and savory (E, F) (results were the mean of 6 replicates, bars represent standard deviation).

Figure 3. Cumulative transport and TEER cell monolayer measurements of rosmarinic acid loaded chitosan-based nanoparticles and free in solution across HCE-T model cells (Values were means of 6 replicates, bars represent standard deviation).

Figure 4. Cumulative transport and TEER cell monolayer measurements of rosmarinic acid loaded chitosan-based nanoparticles and free in solution across ARPE-19 model cells (Values were means of 6 replicates, bars represent standard deviation).

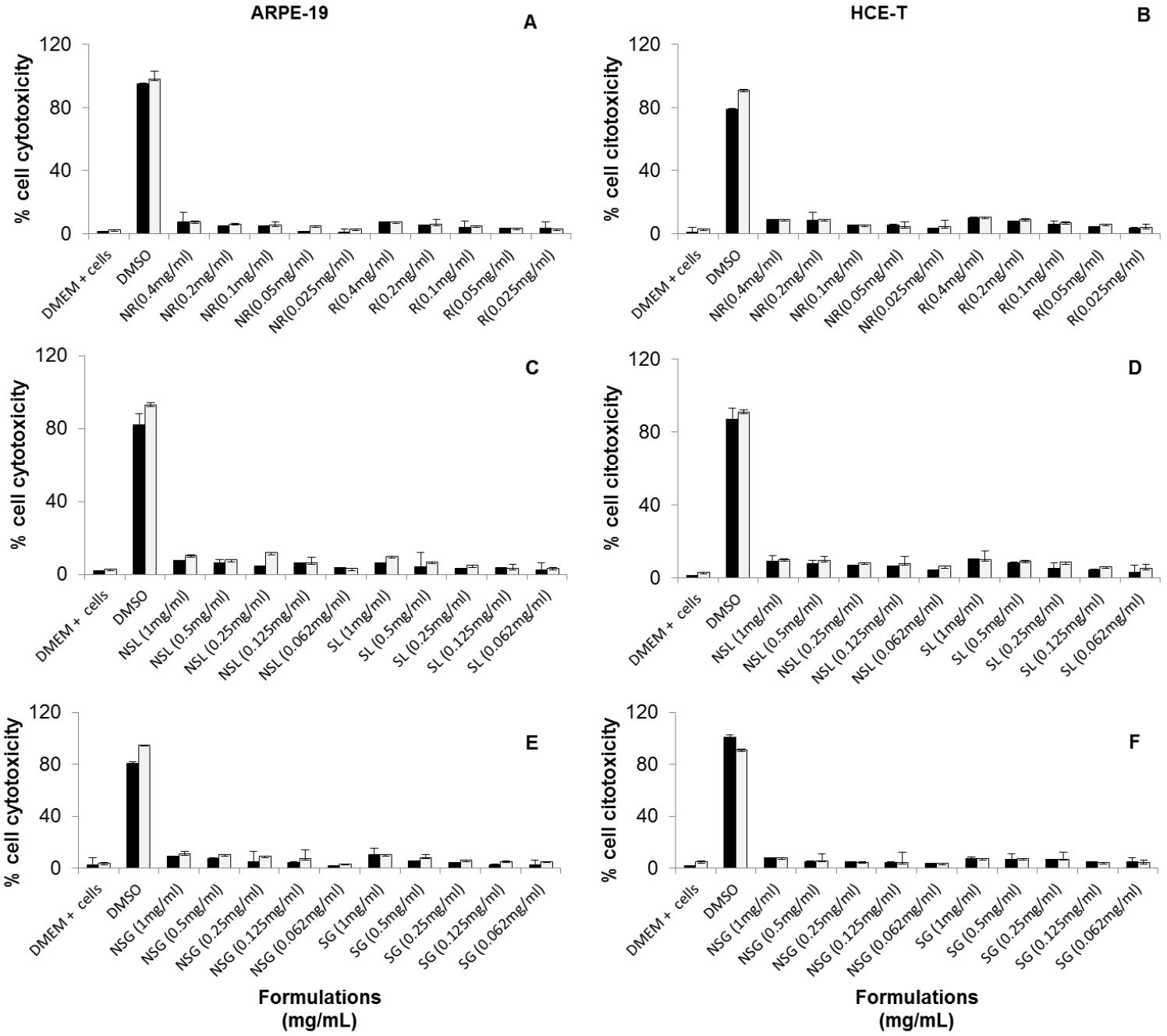

Note: NR, R - rosmarinic acid loaded and unloaded chitosan nanoparticles, respectively; NSL, SL – *Salvia officinalis* loaded and unloaded chitosan nanoparticles, respectively; NSG, SG – *Satureja montana* loaded and unloaded chitosan nanoparticles, respectively.

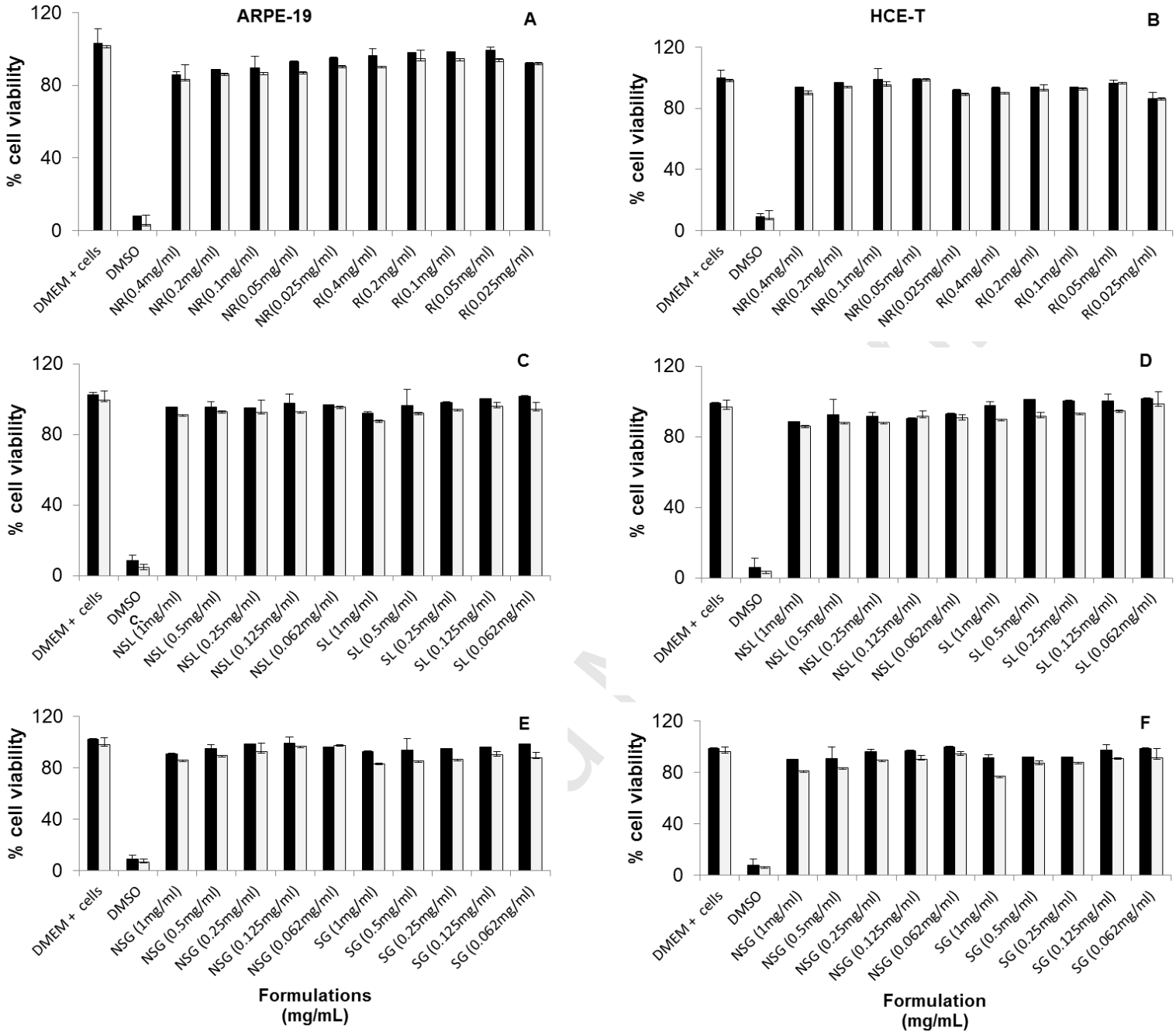

Note: NR, R - rosmarinic acid loaded and unloaded chitosan nanoparticles, respectively; NSL, SL – *Salvia officinalis* loaded and unloaded chitosan nanoparticles, respectively; NSG, SG – *Satureja montana* loaded and unloaded chitosan nanoparticles, respectively.